

1  
2  
3  
4  
5  
6  
7  
8  
9  
10  
11  
12  
13  
14  
15  
16  
17  
18  
19  
20  
21  
22  
23  
24

## Rheology of mixed alginate-hyaluronan aqueous solutions

Andrea Travan<sup>1</sup>, Simona Fiorentino<sup>2</sup>, Mario Grassi<sup>2</sup>, Massimiliano Borgogna<sup>1</sup>, Eleonora Marsich<sup>3</sup>,  
Sergio Paoletti<sup>1</sup>, and Ivan Donati<sup>1,\*</sup>

<sup>1</sup>Department of Life Sciences, Via Licio Giorgieri 5, <sup>2</sup>Department of Engineering and Architecture,  
Via Valerio 10, <sup>3</sup>Department of Medical, Surgical, and Health Sciences, Piazza dell'Ospitale 1,  
University of Trieste, I-34100 Trieste, Italy.

\* Corresponding Author

Dr. Ivan Donati

e-mail: [idonati@units.it](mailto:idonati@units.it)

tel: +39 040 5588733

25 **Abstract**

26 The present manuscript addresses the description of binary systems of hyaluronan (HA) and  
27 alginate (Alg) in semi-concentrated solution. The two polysaccharides were completely miscible in  
28 the entire range of relative weight fraction explored at a total polymer concentration of up to 3 %  
29 (w/V). The rheological study encompassed steady flow and mechanical spectra for HA/Alg systems  
30 at different weight fractions with hyaluronan at different molecular weights. These extensive  
31 analyses allowed us to propose a model for the molecular arrangement in solution that envisages a  
32 mutual exclusion between the two polysaccharides even though a clear phase separation does not  
33 occur. This result may have profound implications when biomaterials based on the combination of  
34 alginate and hyaluronan are proposed in the field of biomedical materials.

35

36

37

38

39

40

41

42

43

44

45

46

47

48

49

## 1. Introduction

Alginate is a collective term to describe a family of polysaccharides isolated from brown seaweeds and bacteria [1]. Chemically, alginates are linear copolymers of 1→4 linked β-D-mannuronic acid (M) and its C-5 epimer, α-L-guluronic acid (G), arranged in a blockwise pattern, with homopolymeric regions of M- and G residues, indicated as M-blocks and G-blocks, respectively, interspersed with regions of alternating structure (MG blocks). At around neutral pH, alginate behaves as an anionic polyelectrolyte and as a semi-flexible chain upon reduction of the medium ionic strength. The ability to form stable hydrogels upon treatment with divalent ions, such as calcium ions [2], have resulted in alginates being widely used in industrial applications. In addition, alginates have relevant applications in the field of biomedical materials [3,4] due to their versatility in gel formation which has been exploited for the encapsulation of, for example, the insulin-producing Langerhans islets for the treatment of type I diabetes [5-8]. In fact, the availability of pure and well-characterised alginate samples makes this material an ideal choice for cell microencapsulation.

In addition to cell encapsulation, alginate has been proposed for several other applications in the biomedical field [3]. For example, alginate-based scaffolds containing hydroxyapatite showed structural features similar to those of the trabecular bone [9-12], and in combination with silver nanoparticles, as well as having antimicrobial properties, have shown good osteointegration in *in vivo* models [12].

However, it should be underlined that unmodified alginate shows non-adhesive properties and, as such, it does not favour cell adhesion [13], which is the first step towards cell proliferation and colonisation. For this reason, the addition of bioactive polymers to alginate has been considered as a way to improve its features [14,15].

Hyaluronan (HA), an alternating copolymer composed of β-D-glucuronic acid (GlcA) and β-D-N-acetylglucosamine (GlcNAc), linked in the sequence →4 GlcA1→3 GlcNAc1→ is the simplest

75 glycosaminoglycan and a major constituent of the extracellular matrix (ECM) as a high molar mass  
76 anionic polyelectrolyte component [16]. Apart from its well-known structural role due to the  
77 peculiar chain semi-flexibility, which gives the polymer exceptional viscoelastic behaviour,  
78 hyaluronan shows important biological features. HA has six known surface receptors [17], among  
79 which CD44 and RHAMM are the most well characterised. While both receptors bind HA through  
80 a common binding domain, they differ, to some extent, in the cellular functions: CD44 mediates cell  
81 attachment, HA uptake and degradation while RHAMM mediates cell locomotion in response to  
82 soluble HA [18].

83 The idea of exploiting mixtures of alginate and hyaluronan to develop novel biomaterials has been  
84 pursued by several authors for mesenchymal stem cell encapsulation [19], as a post-surgical tissue  
85 adhesion barrier [20] and for the encapsulation of chondrocytes [21]. The combination of alginate  
86 and hyaluronan has also been proposed for cartilage engineering by Lindenhayn and co-workers  
87 [22]. In this paper, it was noted that hyaluronan was, to some extent and depending on the alginate  
88 gelation conditions, excluded from the hydrogel network. In addition, Park *et al.* prepared  
89 hyaluronan beads starting from its mixture with alginate and exploiting the ability of the latter to  
90 form “reversible” calcium hydrogels [23]. Most of the above mentioned papers focused on the  
91 biological properties exerted by the mixed construct, but they overlook the physical-chemical  
92 implications incidental to the presence of two anionic polyelectrolytes in solution, which might  
93 impact properties such as gel formation kinetics, stability and mechanical performance.

94

95

96

97

98

99

## 100 2. Materials and Methods

101 Alginate (Alg) (LVG,  $M_W = 120000$ ;  $F_G = 0.69$ ;  $F_{GG} = 0.59$ ;  $N_{G>1} = 16.3$ ;  $PI = 1.9$ ) and hyaluronan  
102 (HA) with  $M_W$  of 1500000 (HA150;  $PI = 2.2$ ) and of 800000 (HA80;  $PI = 2.4$ ) were kindly  
103 provided by FMC, Drammen (Norway). Hyaluronan with a  $M_W$  of 240000 (HA24) was kindly  
104 provided by Sigea S.r.L., Trieste (Italy). Hyaluronan with  $M_W$  of 400000 (HA40;  $PI = 2.7$ ) was  
105 obtained by acid degradation of HA150 according to a procedure previously reported [24] and the  
106 molar mass was evaluated from intrinsic viscosity measurements [25]. In alginate characterization,  
107  $F_G$  denotes the fraction of alginate consisting of guluronic acid,  $F_{GG}$  indicates the fraction of  
108 alginate consisting of guluronic acid in blocks and  $N_{G>1}$  denotes the average length of guluronic  
109 acid blocks. Binary mixtures of HA and Alg were prepared in the presence of aqueous 0.15 M NaCl  
110 at a different weight ratio of HA ( $\phi_{HA}$ ) and of alginate ( $\phi_{Alg} = 1 - \phi_{HA}$ ).

111

### 112 2.1 Viscometry

113 Specific viscosity was measured at 25 °C by means of a Schott-Geräte AVS/G automatic measuring  
114 apparatus and an Ubbelohde-type capillary viscometer in aqueous 0.15 M NaCl. For the  
115 polysaccharides used in the present study, the intrinsic viscosity ( $[\eta]$ ) values were determined by  
116 analyzing the polymer concentration dependence of the reduced specific viscosity ( $\eta_{sp}/c$ ) and of  
117 the logarithm of the reduced relative viscosity ( $\ln(\eta_{rel})/c$ ) by means of the Huggins (eq. 1) and  
118 Kraemer (eq. 2) equations, respectively.

$$119 \frac{\eta_{sp}}{c} = [\eta] + k'[\eta]c \quad (1)$$

$$120 \frac{\ln(\eta_{rel})}{c} = [\eta] - k''[\eta]c \quad (2)$$

121 where  $k'$  and  $k''$  are the Huggins and Kraemer constants, respectively. The specific viscosity of the  
122 Alg/HA mixed solutions was measured in aqueous 0.15 M NaCl at different polysaccharide weight  
123 fractions maintaining a constant total polymer concentration of 1 g/L.

124

## 125 *2.2 Rheological determination*

126 Rheological tests were performed on mixed solutions of alginate and hyaluronan under continuous  
127 shear conditions to determine steady viscosity values in the stress range 1 to 100 Pa, as well as  
128 under oscillatory shear conditions to determine the extension of the linear viscoelasticity regime  
129 (stress sweep tests at 1 Hz in the stress range  $1 < \tau < 500$  Pa) and the mechanical spectra (frequency  
130 sweep,  $\tau = 4$  Pa, within the linear viscoelastic range). The complex viscosity ( $\eta^*$ ), the storage ( $G'$ )  
131 and loss ( $G''$ ) moduli of the binary mixtures and of the hydrogels were recorded in the frequency  
132 range 0.1 – 50 Hz. All tests were carried out with the controlled stress rheometer Rheostress Haake  
133 RS 150 operating at 25 °C. A cone-plate CP60/1° geometry was used in all cases. A glass bell  
134 covering the measuring device was used to improve thermal control and limit evaporation.

135

136

137 **3. Results and Discussion**

138 *3.1 Viscosity in dilute and semi-dilute conditions of binary Alg/HA mixtures*

139 The (macroscopic) mutual compatibility of alginate (Alg) and hyaluronan in dilute binary solution  
140 was assessed by both transmittance measurements and viscometry. In the presence of aqueous NaCl  
141 (0.15 M), the former technique showed no notable variation in the transmittance of the binary  
142 system with respect to that displayed by the polysaccharides alone, thereby excluding the formation  
143 of macroscopic phase separation (data not reported). The complete macroscopic miscibility of the  
144 two polysaccharides was confirmed by the dependence of the specific viscosity of the HA/Alg  
145 dilute binary mixtures on their composition (Figure 1).

146

147 **Figure 1**

148

149 It can be noticed that the experimental results are in very good agreement with the theoretical  
150 prediction that was calculated assuming that no other interaction, apart from the hydrodynamic  
151 ones, occurred between the two polysaccharides [26].

152 The characterisation of HA/Alg binary mixtures was carried out in semi-concentrated solutions by  
153 means of a rheological measurements. The flow curves of the systems under analysis were recorded  
154 in 0.15 M NaCl aqueous solution while varying the weight fraction ( $\phi$ ) of the two polysaccharides  
155 and the molecular weight of the hyaluronan samples. In all cases, a pseudo-plastic behavior was  
156 detected with a clear Newtonian plateau for low values of the shear stress applied. The experimental  
157 curves were fitted with a simplified version of the Cross equation (eq. 3):

158 
$$\eta = \eta_{\dot{\gamma} \rightarrow \infty} + \frac{\eta_0 - \eta_{\dot{\gamma} \rightarrow \infty}}{1 + (k\dot{\gamma})^n} = \frac{\eta_0}{1 + (k\dot{\gamma})^n} \quad (3)$$

159 where  $\eta_{\dot{\gamma} \rightarrow \infty}$ , the viscosity at infinite shear rate, was set equal to zero.  $\eta_0$  is the zero-shear viscosity,  
160 corresponding to the limiting Newtonian plateau for  $\dot{\gamma} \rightarrow 0$ , and  $k$  is the characteristic polymer  
161 relaxation time, often indicated with  $\tau$  [27].  $\tau$  is the time associated with large-scale motion in the  
162 structure of the polymer.  $n$  is known as the Cross Rate Constant and it can be considered as a  
163 “pseudoplasticity index” [28]. The dependence of the zero-shear viscosity on the molecular weight  
164 of hyaluronan for both the polysaccharide alone and for binary HA/Alg mixtures is reported in  
165 Figure 2a, showing a power-law dependence ( $\eta_0 \propto MW^\beta$ ) when the total polysaccharide  
166 concentration was maintained equal to 30 g/L.

167

168

## Figure 2

169

170 In particular, when hyaluronan alone was considered, the power-law dependence showed a scaling  
171 factor of approximately 3.1. This is close to the value (3.4) predicted [29] and reported for different  
172 flexible polysaccharides including hyaluronan [30] and alginate [31] in the semi-dilute regime.  
173 Upon addition of alginate to the system, the scaling factor  $\beta$  showed a non-linear decrease upon  
174 reduction of the fraction of HA in the mixture (Figure 2, inset). This result likely stemmed from the  
175 dilution of hyaluronan due to the addition of the second polysaccharide, *i.e.*, alginate. In fact, the  $\beta$   
176 exponent decreases for all (saccharidic) polymers at lower concentrations, down to the value of 1 in  
177 very dilute conditions. The effect on overall viscosity of the binary system due to the presence of  
178 alginate was also evident from the zero-shear viscosity which was 36.2 Pa·s for  $C_{HA}=15$  g/L and  
179 increased to 84.9 Pa·s in the  $\phi_{HA} = 0.5$  mixture (still with  $C_{HA}=15$  g/L).

180 In Figure 2b, the dependence of the relaxation time,  $\tau$ , on the molecular weight of HA is reported  
181 for both hyaluronan alone and for HA/Alg binary mixtures. In the first case, a power-law of  
182  $\tau \propto MW^{3.5}$  was found, which is very close to the theoretically expected relationship (3.4) [32-34].

183 Similarly, in the case of the binary hyaluronan/alginate mixtures, the exponent of the power law  
184 was 3.2, which is even closer to some reported experimental values of  $\tau$  for HA (3.0) [32-34]. In  
185 Figure 3a the dependence of the zero-shear viscosity for the binary Alg/HA mixtures on the weight  
186 fraction of HA ( $\phi_{\text{HA}}$ ) is reported for HA at different values of the molecular weight.

187

188

### Figure 3

189

190 It can be seen that in all cases, a scaling law holds, at least in the  $\phi_{\text{HA}}$  range explored. In Figure 3b  
191 and 3c, the dependence of the zero-shear viscosity and of the polymer relaxation time,  $\tau$ , on the  
192 concentration of HA is reported for both a hyaluronan solution alone and a HA/Alg binary mixture  
193 with  $\phi_{\text{HA}} = 0.50$ . For both properties, the addition of alginate brings about an effect that differs from  
194 that of the pure dilution with the solvent. This provides an indication of the arrangement between  
195 the two components of the mixture at a molecular level. In fact, considering the onset of the shear-  
196 thinning behavior as a progressive decrease in the steady-state entanglements density of the  
197 hyaluronan chains [33], the higher  $\tau$  in the presence of alginate seems to point to an effective  
198 higher concentration of HA which might arise from a (at least partial) segregation, rather than its  
199 homogeneous mixing with alginate.

200

### 201 *3.2 Mechanical spectroscopy*

202 The stress sweep curves for the samples were recorded and a type I behavior was found in all cases.  
203 A typical curve is reported in Figure 4 together with the best fit of the experimental data according  
204 to the Soskey-Winter equation (eq. 4).

205

206

207 
$$G' = G'_0 \frac{1}{1 + (b\gamma)^n} \quad (4)$$

208 Where  $\gamma$  is the strain,  $G'_0$  is the limiting value of the storage modulus for  $\gamma \rightarrow 0$ , while  $b$  and  $n$  are  
 209 adjustable parameters. The critical strain,  $\gamma_c$ , marking the limit of the linear viscoelastic regime,  
 210 was arbitrarily assumed to correspond to  $G'/G'_0 = 0.95$ . The limit of the linear viscoelastic response  
 211 is reported in table 1.

212

213 **Figure 4**

214

215 **Table 1**

216

217 The mechanical response of hyaluronan alone and of its binary mixtures with alginate was recorded  
 218 as a function of pulsation,  $\omega$  ( $= 2\pi\nu$ ). Depending on the molecular weight of hyaluronan, a  
 219 transition from viscous ( $G'' > G'$ ) to elastic ( $G' > G''$ ) behaviour took place in the frequency range  
 220 explored (Figure 5a, for the sample case of HA150) with a cross-over point.

221

222 **Figure 5**

223

224 The experimental data were fitted using a generalised Maxwell model composed of a sequence of  
 225 elements in parallel (spring and dashpot). The frequency dependence of the viscous ( $G'$ ) and elastic  
 226 ( $G''$ ) response is then described with the following equations (eqs. 5 and 6):

227 
$$G' = \sum_{i=1}^n G_i \frac{(\lambda_i \omega)^2}{1 + (\lambda_i \omega)^2} \quad (5)$$

228 
$$G'' = \sum_{i=1}^n G_i \frac{\lambda_i \omega}{1 + (\lambda_i \omega)^2} \quad \text{with} \quad G_i = \eta_i / \lambda_i \quad (6)$$

229 where  $n$  is the number of Maxwell elements considered,  $G_i$ ,  $\eta_i$  and  $\lambda_i$  represent the spring constant,  
 230 the dashpot viscosity and the relaxation time of the  $i$ th Maxwell element, respectively [35]. The  
 231 fitting of the experimental data was performed assuming that the relaxation times were not  
 232 independent of each other but they were scaled by a factor 10. The number of Maxwell elements  
 233 was selected, based on a statistical procedure, to minimise the product  $\chi^2 N_p$ , where  $\chi^2$  is the sum of  
 234 the squared errors, while  $N_p (= 2 + n)$  indicates the number of fitting parameters (table 2).

235

236

### Table 2

237

238 Figure 5b reports the dependence of the frequency corresponding to the cross-over point,  $\omega_{\text{cross}}$  ( $=$   
 239  $2\pi\nu_{\text{cross}}$ ), on the molecular weight of hyaluronan for both HA alone and for its binary mixtures with  
 240 alginate. In both cases, a very similar power-law relation holds for HA alone and for the HA/Alg  
 241 mixture, namely  $\omega_{\text{cross}} \propto MW^{-3.1}$  and  $\omega_{\text{cross}} \propto MW^{-3.2}$ , respectively. This is in good agreement with  
 242 the experimental findings reported in the literature for hyaluronan solutions [36]. Despite the  
 243 increase in  $\omega_{\text{cross}}$  determined by the dilution of hyaluronan with alginate, it appears that the  
 244 entangled structure was not altered, with respect to the dilution of hyaluronan alone, by the presence  
 245 of alginate. However, in the case of the HA sample with the highest molecular weight, the  
 246 mechanical response of the binary mixture was also compared with a solution containing only  
 247 hyaluronan at the same concentration as in the mixture (Figure 5b, triangle). It can be noted that in  
 248 this latter case, the  $\omega_{\text{cross}}$  is higher than that of the mixture.

249 Figure 5c reports the dependence of the modulus-at-cross-over,  $G_{\text{cross}}$  ( $G_{\text{cross}} \equiv G'_{\text{cross}} = G''_{\text{cross}}$ ), on the  
 250 molecular weight of HA. It can be seen that in the case of hyaluronan alone, a power-law

251 dependence  $G_{cross} \propto MW_{HA}^{-0.1}$  holds, which is in good accordance with the experimental results  
252 previously reported for hyaluronan, *i.e.*  $G_{cross} \propto MW^0$  [36]. In contrast, when alginate is added to  
253 HA to form the binary system,  $G'$  and  $G''$  show a non-zero (negative) dependence on the molecular  
254 weight of hyaluronan - more specifically,  $G_{cross} \propto MW^{-1.2}$ . It follows that the presence of the  
255 second polysaccharide brings about interference on the viscoelastic properties of the binary system  
256 whose extent is dependent on the molecular weight of the hyaluronan used in the system.  
257 Figure 6 shows the relative effect on  $\eta_0$  and  $\omega_{cross}$  due to the dilution of a hyaluronan solution with  
258 the solvent and of a HA/Alg binary mixture with  $\phi_{HA} = 0.5$ .

259

260

### Figure 6

261

262 In relative terms, the variation of  $\omega_{cross}$  was more marked in the case of the mixture than of the HA  
263 alone while basically no effect was noted on  $\eta_0$ . This behaviour indicates that alginate lacks specific  
264 interactions with hyaluronan and contributes to the viscosity in simply additive terms. At variance,  
265 alginate markedly affects the formation of the complex network of entanglement which is the basis  
266 for the mechanical response of HA containing systems.

267

### 4. Conclusion

268  
269 The biotechnological relevance of polysaccharide mixtures as ECM mimics has gained attention  
270 over recent years. However, while mixed systems have been exploited for *in-vitro* experiments,  
271 extended physical-chemical analyses are still partially lacking.

272 The present manuscript deals with the experimental physical-chemical characterisation by rotational  
273 rheometry of binary mixtures of alginate and hyaluronan. These analyses allow us to propose a  
274 model for the mutual arrangement of the two polysaccharides in solution that envisages a situation

275 where the polyanions tend to segregate instead of mixing freely, but without leading to macroscopic  
276 phase separation. These results may impact systems in which a three-dimensional arrangement  
277 (hydrogel), for biological purposes where a controlled release of the biologically active component  
278 might affect the final outcome. Rheological measurements in semi-dilute solution provide new  
279 information on the system at the macroscopic level and have shown that, although the combined  
280 presence of the two polysaccharides does not give rise to marked synergistic effects, alginate and  
281 hyaluronan tends to exclude each other, thus forming microdomains enriched in the two separate  
282 components instead of a true homogeneous one-phase solution. This conclusion has notable  
283 implications for systems using hydrogel formations. In fact, the treatment of the binary mixtures  
284 with calcium ions, although leading to a three dimensional architecture due to the presence of  
285 alginate, could result in an uneven distribution of the two components where hyaluronan might be  
286 excluded from the three dimensional structure and may be confined at the borders of the hydrogel  
287 [22]. The present manuscript will be followed by another work where the formation and mechanical  
288 properties of hydrogels from mixed systems of alginate and hyaluronan, together with their  
289 biological properties, will be explored.

290

## 291 **Acknowledgments**

292 This study was supported by the EU-FP7 Project “Development of a resorbable sealing patch for  
293 the prevention of anastomotic leakage after colorectal cancer surgical treatment - AnastomoSEAL”  
294 (Contract number 280929) and by the Italian Ministry of Education (PRIN 2010-11  
295 (20109PLMH2)).

296

297

298

299

300 **Captions to Figures**

301

302 **Figure 1.** Dependence of the reduced specific viscosity from mixture composition for HA/Alg  
303 systems at total polymer concentration of 1 g/L in aqueous 0.15M NaCl. The dotted line represents  
304 the theoretical dependence based on Donati et al [26].

305

306 **Figure 2.** Dependence of the zero-shear viscosity ( $\eta_0$ , **a**) and relaxation time ( $k$ , **b**) on HA  
307 molecular weight (MW) for hyaluronan alone ( $\blacksquare$ ) and for HA-Alg binary mixtures with  $\phi_{\text{HA}} = 0.5$   
308 ( $\square$ ). In **a**,  $\blacktriangle$  represents a hyaluronan solution at a total polymer concentration of 15 g/L and  $\triangle$   
309 represents the theoretical value of zero-shear viscosity calculated for a HA-Alg binary mixtures  
310 with  $\phi_{\text{HA}} = 0.5$  according to [26]. Inset in **a**: Dependence of the scaling factor  $\beta$  ( $\eta_0 \propto MW^\beta$ ) on the  
311 fraction of HA in the HA/Alg binary mixture. In all cases, total polymer concentration = 30 g/L.

312

313 **Figure 3.** **a)** Dependence of the zero-shear viscosity,  $\eta_0$ , on hyaluronan fraction ( $\phi_{\text{HA}}$ ) for binary  
314 mixtures with alginate of HA150 ( $\blacksquare$ ), HA80 ( $\square$ ) and HA40 ( $\bullet$ ). **b)** Dependence of the zero shear  
315 viscosity,  $\eta_0$ , on hyaluronan concentration ( $C_{\text{HA}}$ ) of a HA solution upon addition of alginate at  
316 constant total polymer concentration of 30 g/L ( $\blacksquare$ ), or upon dilution ( $\square$ ). **c)** Dependence of the  
317 polymer-chain relaxation time,  $k$ , on hyaluronan concentration ( $C_{\text{HA}}$ ) of a HA solution upon  
318 addition of alginate at constant total polymer concentration of 30 g/L ( $\blacksquare$ ), or upon dilution ( $\square$ ).

319

320 **Figure 4.** Example of a stress sweep ( $G'$ ) test for a mixture of hyaluronan and alginate ( $\blacksquare$ ). Dotted  
321 line represents the best fit of the experimental data according to the Soskey-Winter equation (eq. 5).

322

323 **Figure 5. a)** Dependence of the storage ( $G'$ , ■) and loss ( $G''$ , □) moduli from the pulsation,  $\omega$  (=   
324  $2\pi\nu$ ), for a HA/Alg binary solution, with hyaluronan weight fraction  $\phi_{\text{HA}} = 0.5$  (sample HA150).   
325 Solid and dotted lines represent generalised Maxwell model best fitting (eq. 5 and 6). **b)**   
326 Dependence of the cross-over pulsation on molecular weight of hyaluronan for HA alone (■) and   
327 HA/Alg binary solutions with  $\phi_{\text{HA}} = 0.5$  (□). In both cases, total polysaccharide concentration was   
328 30 g/L. Parenthesis indicate  $\omega_{\text{cross}}$  values outside the frequency range explored and calculated with   
329 eqs. 5 and 6. In **b)**, ▲ represents the pulsation corresponding to cross-over for a HA solution of 15   
330 g/L. **c)** Dependence on the molecular weight of HA of the elastic ( $G'$ ) and viscous ( $G''$ ) modulus at   
331 the cross-over point for a hyaluronan solution alone (■) and for a HA/Alg binary solution with  $\phi_{\text{HA}}$    
332 = 0.5 (□). All solutions were prepared in aqueous 0.15 M NaCl.

333

334 **Figure 6.** Relative variation of zero shear viscosity ( $\eta_{0c}/\eta_{0c=30\text{g/L}}$ ) with total polymer concentration   
335 ( $C_{\text{Tot}} = C_{\text{HA}} + C_{\text{Alg}}$ ) (right y-scale) for HA (■) and HA/Alg mixture (□,  $\phi_{\text{HA}} = 0.5$ ) upon dilution   
336 with solvent (0.15 M NaCl). Relative dependence of the pulsation corresponding to the crossover (   
337  $\omega_{\text{cross},c}/\omega_{\text{cross},c=30\text{g/L}}$ ) on total polymer concentration (left y-scale) for HA (●) and for the HA/Alg   
338 mixture (○,  $\phi_{\text{HA}} = 0.5$ ).

339

340

341

342

343 **References**

- 344 1. I. Donati, S. Paoletti, Material Properties of Alginates, in: B.H.A. Rhem (Eds), Alginates;  
345 Biology and Applications, Springer-Verlag, Berlin Heidelberg, 2009, pp. 1-53.
- 346 2. K.I. Draget, O. Smidsrød, G. Skjåk-Bræk, Alginates from algae, in: A. Steinbüchel, S.K.  
347 Rhee (Eds), Polysaccharides and Polyamides in the Food Industry. Properties,  
348 Production, and Patents., Wiley-VCH Verlag GmbH & Co., Weinheim, 2005, pp. 1-  
349 30.
- 350 3. T.H. Silva, A. Alves, B.M. Ferreira, J.M. Oliveira, L.L. Reys, R.J.F. Ferreira, R.A. Sousa,  
351 S.S. Silva, J.F. Mano, R.L. Reis, Materials of marine origin: A review on polymers  
352 and ceramics of biomedical interest, *Int. Mater. Rev.* 57 (2012) 276-307.
- 353 4. S. Van Vlierberghe, P. Dubruel, E. Schacht, Biopolymer-based hydrogels as scaffolds for  
354 tissue engineering applications: A review, *Biomacromolecules* 12 (2011) 1387-1408.
- 355 5. R. Calafiore, G. Basta, G. Luca, A. Lemmi, M.P. Montanucci, G. Calabrese, L. Racanicchi,  
356 F. Mancuso, P. Brunetti, Microencapsulated pancreatic islet allografts into  
357 nonimmunosuppressed patients with type 1 diabetes: first two cases, *Diabetes Care*  
358 29 (2006) 137-138.
- 359 6. P. de Vos, M.M. Faas, B. Strand, R. Calafiore, Alginate-based microcapsules for  
360 immunoisolation of pancreatic islets, *Biomaterials* 27 (2006) 5603-5617.
- 361 7. P. de Vos, M. Bucko, P. Gemeiner, M. Navrátil, J. Švitel, M. Faas, B.L. Strand, G. Skjåk-  
362 Bræk, Y.A. Mørch, A. Vikartovská, I. Laciík, G. Kolláriková, G. Orive, D. Poncetlet,  
363 J.L. Pedraz, M.B. Ansorge-Schumacher, Multiscale requirements for  
364 bioencapsulation in medicine and biotechnology, *Biomaterials* 30 (2009) 2559-2570.
- 365 8. F. LimA.M. Sun, Microencapsulated islets as bioartificial endocrine pancreas, *Science* 210  
366 (1980) 908-910.
- 367 9. G. Turco, E. Marsich, F. Bellomo, S. Semeraro, I. Donati, F. Brun, M. Grandolfo, A.  
368 Accardo, S. Paoletti, Alginate/hydroxyapatite biocomposite for bone ingrowth: A  
369 trabecular structure with high and isotropic connectivity, *Biomacromolecules* 10  
370 (2009) 1575-1583.
- 371 10. G. Jin, G. Kim, Multi-layered polycaprolactone-alginate-fucoidan biocomposites  
372 supplemented with controlled release of fucoidan for bone tissue regeneration:  
373 Fabrication, physical properties, and cellular activities, *Soft Matter* 8 (2012) 6264-  
374 6272.
- 375 11. C.C. Yu, J.J. Chang, Y.H. Lee, Y.C. Lin, M.H. Wu, M.C. Yang, C.T. Chien, Electrospun  
376 scaffolds composing of alginate, chitosan, collagen and hydroxyapatite for applying  
377 in bone tissue engineering, *Mater. Lett.* 93 (2013) 133-136.
- 378 12. E. Marsich, F. Bellomo, G. Turco, A. Travan, I. Donati, S. Paoletti, Nano-composite  
379 scaffolds for bone tissue engineering containing silver nanoparticles - preparation,

- 380 characterization and biological properties, *J. Mater. Sci-Mater. M.* 24 (2013) 1799-  
381 1807.
- 382 13. A.D. Augst, H.J. Kong, D.J. Mooney, Alginate Hydrogels as Biomaterials, *Macromol.*  
383 *Biosci.* 6 (2006) 623-633.
- 384 14. E. Marsich, M. Borgogna, I. Donati, P. Mozetic, B.L. Strand, S.G. Salvador, F. Vittur, S.  
385 Paoletti, Alginate/lactose-modified chitosan hydrogels: a bioactive biomaterial for  
386 chondrocyte encapsulation, *J. Biomed. Mater Res. A* 84 (2008) 364-376.
- 387 15. E. Marsich, A. Travan, M. Feresini, R. Lapasin, S. Paoletti, I. Donati, Polysaccharide-Based  
388 Polyanion-Polycation-Polyanion Ternary Systems in the Concentrated Regime and  
389 Hydrogel Form, *Macromol. Chem. Phys.* 214 (2013) 1309-1320.
- 390 16. C.B. KnudsonW. Knudson, Cartilage proteoglycans, *Semin. Cell Dev. Biol.* 12 (2001) 69-  
391 78.
- 392 17. D.E. Ingber, Mechanical control of tissue morphogenesis during embryological  
393 development, *Int. J. Dev. Biol.* 50 (2006) 255-266.
- 394 18. J. Gailit, R.A.F. Clark, Wound repair in the context of extracellular matrix, *Curr. Opin. Cell*  
395 *Biol.* 6 (1994) 717-725.
- 396 19. E.E. Coates, C.N. Riggin, J.P. Fisher, Photocrosslinked alginate with hyaluronic acid  
397 hydrogels as vehicles for mesenchymal stem cell encapsulation and chondrogenesis,  
398 *J. Biomed. Mater. Res.* 101A (2013) 1962-1970.
- 399 20. S. Oh, S. Na, K. Song, J. Lee, Sprayable powder of hyaluronate embedded in mildly cross-  
400 linked alginate as a post-surgical tissue adhesion barrier, *Macromol. Res.* 2013) 1-7.
- 401 21. C. Gigant-Huselstein, P. Hubert, D. Dumas, E. Dellacherie, P. Netter, E. Payan, J.F. Stoltz,  
402 Expression of adhesion molecules and collagen on rat chondrocyte seeded into  
403 alginate and hyaluronate based 3D biosystems. Influence of mechanical stresses,  
404 *Biorheology* 41 (2004) 423-431.
- 405 22. K. Lindenhayn, C. Perka, R.S. Spitzer, H.H. Heilmann, K. Pommerening, J. Mennicke, M.  
406 Sittinger, Retention of hyaluronic acid in alginate beads: Aspects for in vitro  
407 cartilage engineering, *J. Biomed. Mater. Res.* 44 (1999) 149-155.
- 408 23. K.H. Bae, J.J. Yoon, T.G. Park, Fabrication of hyaluronan acid hydrogel beads for cell  
409 encapsulation, *Biotechnol. Prog.* 22 (2006) 297-302.
- 410 24. K. TømmeraasC. Melander, Kinetics of Hyaluronan Hydrolysis in Acidic Solution at  
411 Various pH Values, *Biomacromolecules* 9 (2008) 1535-1540.
- 412 25. A. Gamini, S. Paoletti, F. Zanetti, Chain rigidity of polyuronates: static light scattering of  
413 aqueous solutions of hyaluronate and alginate, in: S.E. Harding, D.B. Sattelle, V.A.  
414 Bloomfield (Eds), *Laser Light Scattering in Biochemistry*, Royal Society of  
415 Chemistry, Cambridge, 1992, pp. 294-311.

- 416 26. I. Donati, M. Borgogna, E. Turello, A. Cesáro, S. Paoletti, Tuning Supramolecular  
417 Structuring at the Nanoscale Level: Nonstoichiometric Soluble Complexes in Dilute  
418 Mixed Solutions of Alginate and Lactose-Modified Chitosan (Chitlac),  
419 *Biomacromolecules* 8 (2007) 1471-1479.
- 420 27. M.M. Cross, Relation between viscoelasticity and shear-thinning behaviour in liquids,  
421 *Rheol. Acta* 18 (1979) 609-614.
- 422 28. M.M. Cross, Rheology of non-Newtonian fluids: a new flow equation for pseudoplastic  
423 systems, *J. Colloid. Sci.* 20 (1965) 417-437.
- 424 29. P.G. De Gennes, Dynamics of Entangled Polymer Solutions. I. The Rouse Model,  
425 *Macromolecules* 9 (1976) 587-593.
- 426 30. D. Calciu-Rusu, E. Rothfuss, J. Eckelt, T. Haase, H.B. Dick, B.A. Wolf, Rheology of  
427 Sodium Hyaluronate Saline Solutions for Ophthalmic Use, *Biomacromolecules* 8  
428 (2007) 1287-1292.
- 429 31. T. Matsumoto, M. Kawai, T. Masuda, influence of concentration and  
430 mannuronate/guluronate [correction of gluronate] ratio on steady flow properties of  
431 alginate aqueous systems, *Biorheology* 29 (1992) 411-417.
- 432 32. M.K. Cowman, S. Matsuoka, Experimental approaches to hyaluronan structure, *Carbohydr.*  
433 *Res.* 340 (2005) 791-809.
- 434 33. E. Fouissac, M. Milas, M. Rinaudo, Shear-rate, concentration, molecular weight, and  
435 temperature viscosity dependences of hyaluronate, a wormlike polyelectrolyte,  
436 *Macromolecules* 26 (1993) 6945-6951.
- 437 34. W.E. Krause, E.G. Bellomo, R.H. Colby, Rheology of Sodium Hyaluronate under  
438 Physiological Conditions, *Biomacromolecules* 2 (2001) 65-69.
- 439 35. R. Lapasin, S. Pricl, *Rheology of Industrial Polysaccharides, Theory and Applications*,  
440 Chapman and Hall, London, 1995.
- 441 36. M. Milas, M. Rinaudo, I. Roure, S. Al-Assaf, G.O. Phillips, P.A. Williams, Comparative  
442 rheological behavior of hyaluronan from bacterial and animal sources with cross-  
443 linked hyaluronan (hylan) in aqueous solution, *Biopolymers* 59 (2001) 191-204.  
444  
445

**Table 1.** Composition, critical strain and critical stress ( $\tau_c$ ) for binary HA/Alg mixtures in NaCl 0.15 M.  $\phi_{HA}$  represents the weight fraction of hyaluronan in the mixture.

Sample	$\phi_{HA}$	$\gamma_c$	$\tau_c$ (Pa)
HA150 30 g/L	1	0.44	123.3
HA150 22g/L	1	0.50	72.6
HA150 18g/L	1	0.51	45.5
HA150 15g/L	1	0.99	48.3
HA80 30 g/L	1	0.55	107.3
HA40 30 g/L	1	0.79	38.2
HA150/Alg 30 g/L	0.73	0.7	79.5
HA150/Alg 30 g/L	0.6	0.68	77.1
HA150/Alg 30 g/L	0.5	0.58	46.5
HA150/Alg 30 g/L	0.4	0.62	30.3
HA80/Alg 30 g/L	0.73	0.54	61.4
HA80/Alg 30 g/L	0.6	0.64	33.9
HA80/Alg 30 g/L	0.5	0.91	47.0
HA80/Alg 30 g/L	0.4	0.68	21.1
HA40/Alg 30 g/L	0.73	1.0	26.8
HA40/Alg 30 g/L	0.6	0.86	13.2
HA40/Alg 30 g/L	0.5	0.85	16.8
HA150/Alg 25 g/L	0.5	0.59	29.2
HA150/Alg 20 g/L	0.5	0.65	15.0
HA150/Alg 15 g/L	0.5	0.65	6.8

**Table 2.** Parameters obtained from the fitting of the experimental datapoints of the mechanical spectra for the hyaluronan/alginate binary mixture ( $G_i$ ,  $\lambda_i$ ,  $\eta_i$ , eqs. 5 and 6).

Sample	$\phi_{HA}$	$G_i$ (Pa)	$\lambda_i$ (s)	$\eta_i$ (Pa·s)
HA150 30g/L	1	281.2	0.0041	1.2
		288.9	0.0414	11.9
		189.9	0.414	78.6
		62.1	4.14	257.1
HA150 22 g/L	1	202.0	0.0074	1.49
		165.2	0.074	12.2
		77.0	0.739	56.9
		12.7	7.388	93.7
HA150 18 g/L	1	153.2	0.005	0.8
		126.1	0.0504	6.4
		53.1	0.5041	26.8
		9.2	5.0414	46.2
HA150 15 g/L	1	91.8	0.0011	0.1
		94.2	0.0109	1.0
		64.1	0.1093	7.0
		17.3	1.0935	18.9
HA80 30 g/L	1	432.2	0.0045	1.9
		313.3	0.0451	14.1
		110.8	0.4513	49.9
		14.3	4.5513	64.7
HA40 30g/L	1	589.6	0.0006	0.4
		388.4	0.0061	2.4
		85.6	0.0615	5.3
		4.8	0.6147	3.0
HA24 30g/L	1	351.9	0.0001	0.04
		290.8	0.0012	0.3
		54.1	0.012	0.6
		2.8	0.12	0.3

**Table A.2** (continued)

Sample	$\phi_{\text{HA}}$	$G_i$ (Pa)	$\lambda_i$ (s)	$\eta_i$ (Pa·s)
HA150/Alg 30 g/L	0.73	281.1	0.004	1.1
		179.9	0.040	7.2
		112.6	0.399	44.9
		32.1	3.986	128.0
HA150/Alg 30 g/L	0.6	325.4	0.0015	0.5
		168.1	0.0153	2.6
		112.0	0.1533	17.2
		43.3	1.5333	66.3
HA150/Alg 30 g/L	0.5	256.4	0.004	1.1
		107.2	0.041	4.4
		53.4	0.412	22.0
		11.2	4.119	46.2
HA150/Alg 30 g/L	0.4	385.5	0.0013	0.5
		96.3	0.0129	1.2
		51.7	0.1292	6.7
		15.4	1.2924	19.8
HA80/Alg 30 g/L	0.73	506.1	0.001	0.5
		295.9	0.009	2.9
		157.3	0.098	15.4
		29.6	0.976	28.9
HA80/Alg 30 g/L	0.6	325.3	0.003	1.0
		124.0	0.031	3.9
		29.6	0.313	9.3
		1.9	3.129	6.0
HA80/Alg 30 g/L	0.5	329.6	0.003	1.1
		120.4	0.032	3.9
		30.5	0.322	9.8
		2.3	3.218	7.4
HA80/Alg 30 g/L	0.4	393.2	0.0006	0.3
		172.8	0.006	1.1
		51.7	0.064	3.3
		6.9	0.644	4.5

**Table A.2** (continued)

Sample	$\phi_{\text{HA}}$	$G_i$ (Pa)	$\lambda_i$ (s)	$\eta_i$ (Pa·s)
HA40/Alg 30 g/L	0.73	478.1	0.002	1.0
		111.3	0.021	2.3
		8.8	0.206	1.8
		0.2	2.064	0.4
HA40/Alg 30 g/L	0.6	386.9	0.002	0.9
		54.5	0.023	1.3
		3.2	0.236	0.7
		0.01	2.357	0.03
HA40/Alg 30 g/L	0.5	481.7	0.002	1.2
		66.3	0.024	1.6
		4.1	0.244	1.0
		0.07	2.436	0.2
HA150/Alg 25 g/L	0.5	287.0	0.001	0.4
		95.0	0.012	1.2
		55.7	0.122	6.8
		16.4	1.222	20.1
HA150/Alg 20 g/L	0.5	280.9	0.0008	0.2
		46.3	0.008	0.4
		33.3	0.082	2.7
		8.2	0.825	6.7

Figure 1

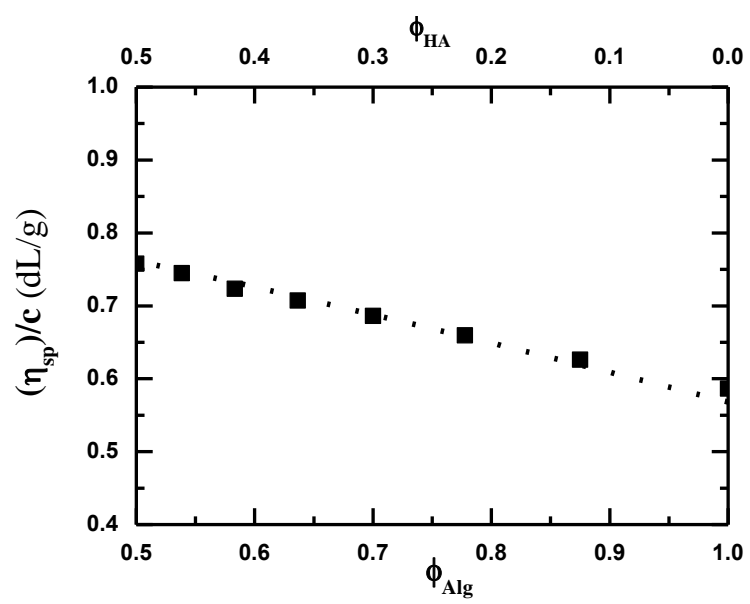


**Figure 2**

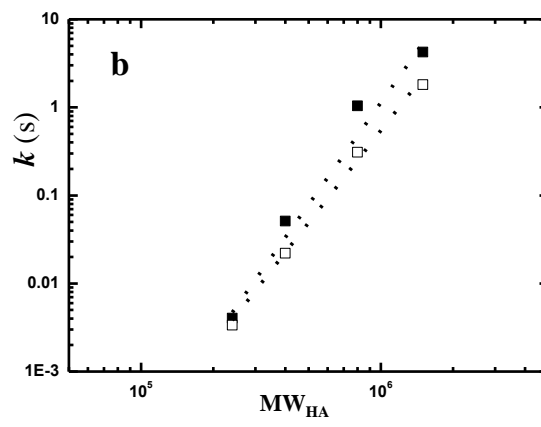
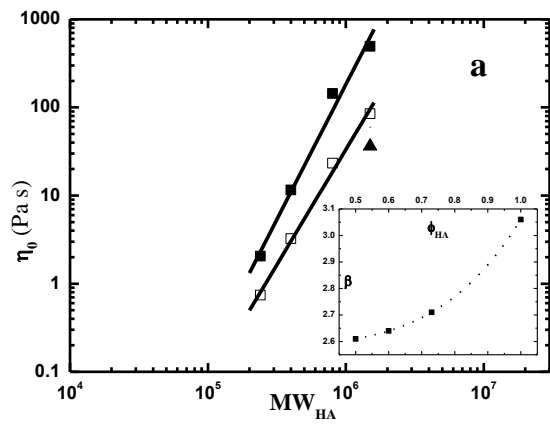


Figure 3

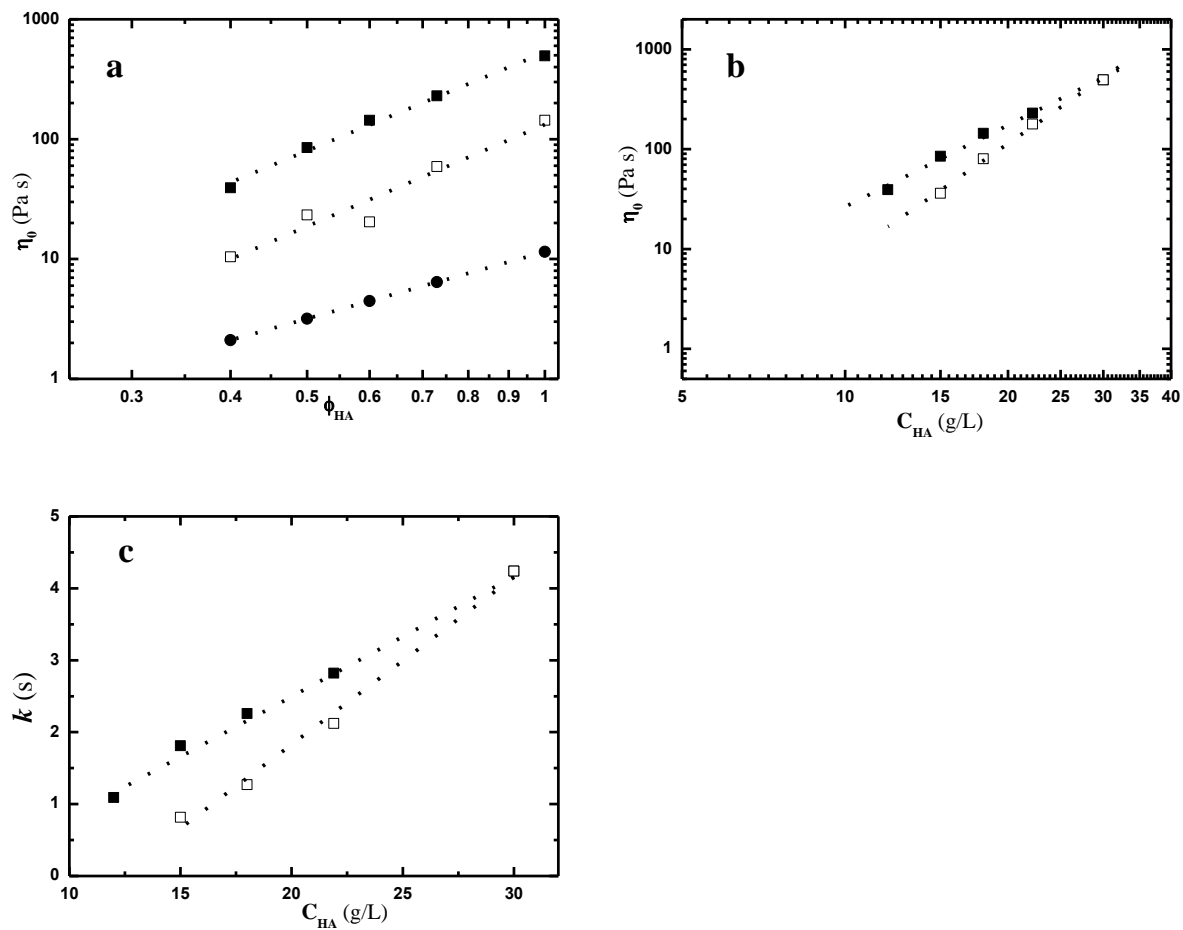


Figure 4

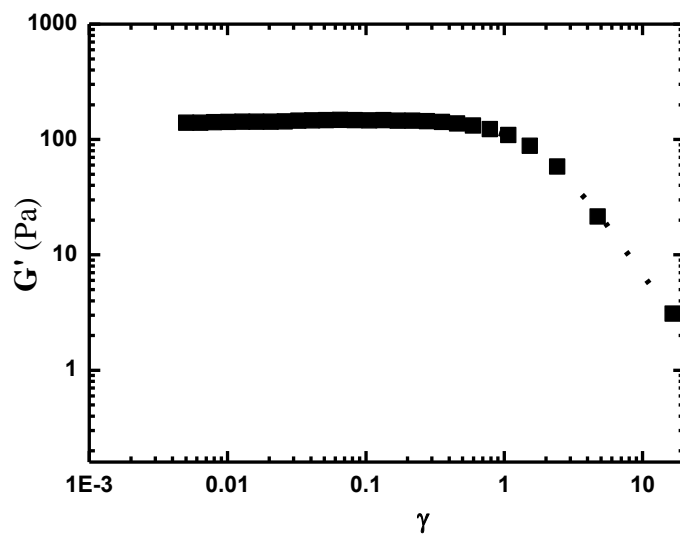


Figure 5

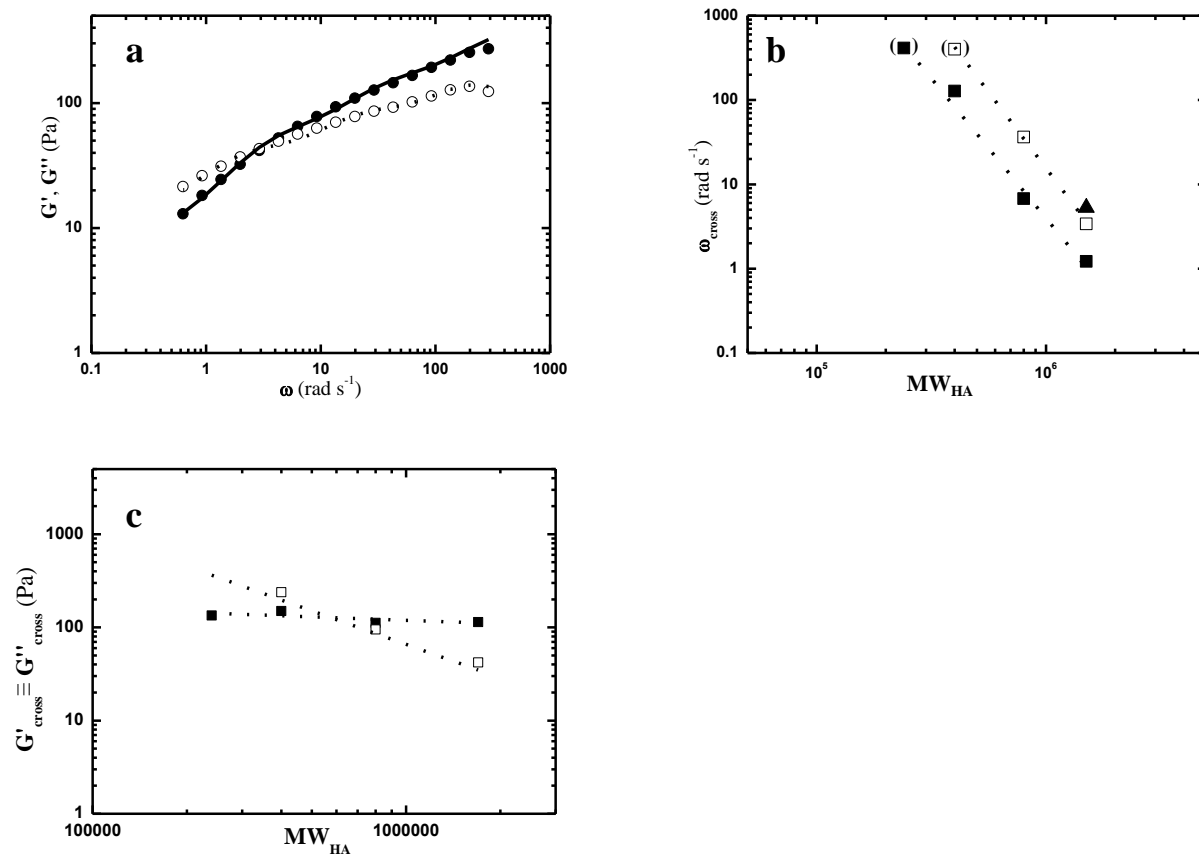


Figure 6

